Electronic Supplementary Material (ESI) for Nanoscale.

Supporting Information

Nanoparticles induced chemoresistance: The emerging modulatory effects of engineered nanomaterials on human intestinal cancer cells redox metabolic adaptation

Zhuoran Wu,[‡a] Magdiel Inggrid Setyawati,[‡a] Hong Kit Lim,[a] Kee Woei Ng,[abc] Chor Yong Tay*[ab]

[a]School of Materials Science and Engineering, Nanyang Technological University, 50 Nanyang Avenue, Singapore 639798, Singapore.
[b]Environmental Chemistry and Materials Centre, Nanyang Environment & Water Research Institute, 1 Cleantech Loop, CleanTech One, Singapore 637141, Singapore.
[c]Center for Nanotechnology and Nanotoxicology, Department of Environmental Health, Harvard T.H. Chan School of Public Health, Boston, MA 02115, USA.

‡These authors contributed equally to this work.

*Corresponding author: Chor Yong Tay (cytay@ntu.edu.sg)

Supplementary Figures

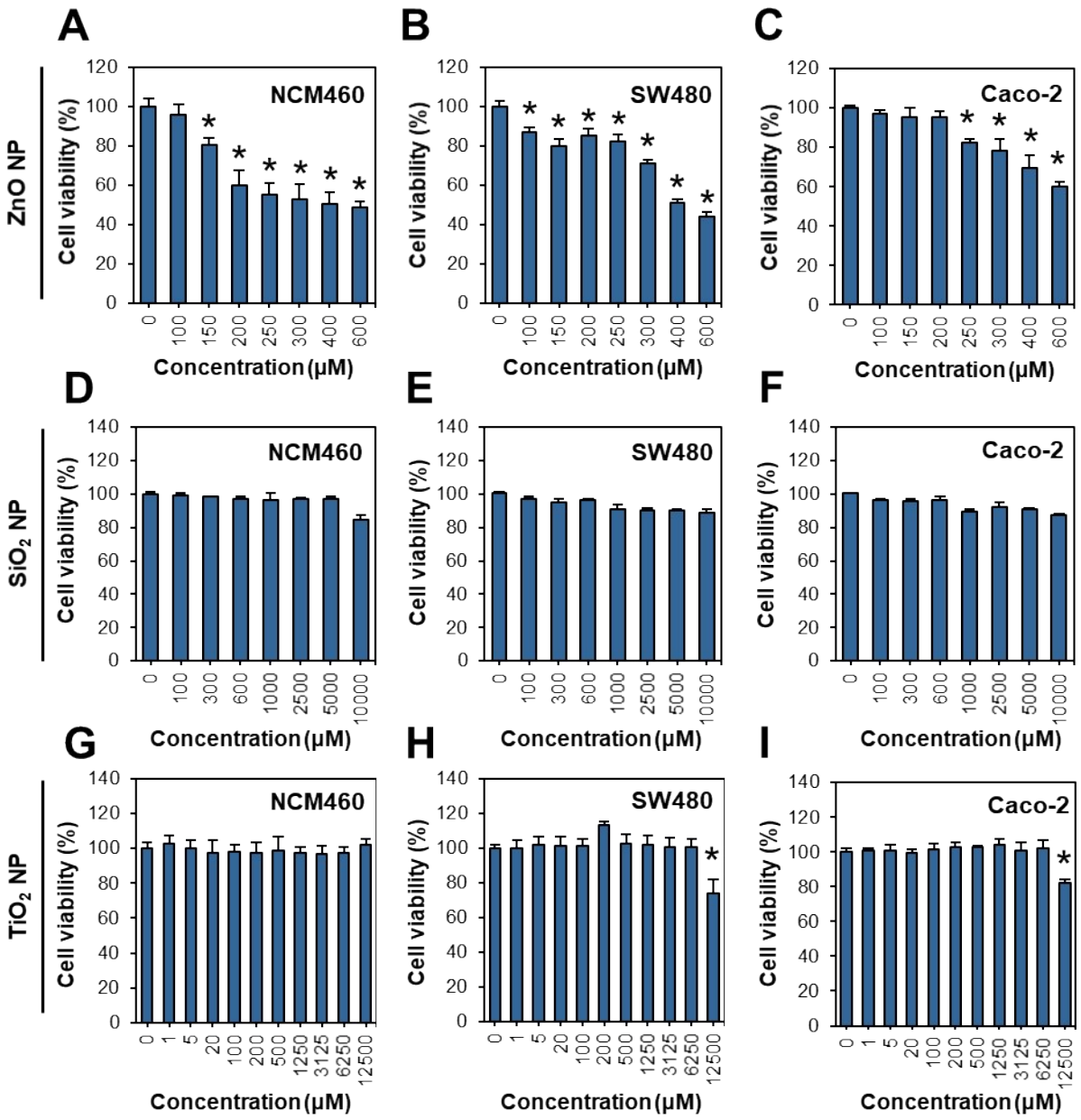

Figure S1. Dose-response curves of (**A-C**) ZnO NPs, (**D-E**) SiO_2 NPs and (**G-I**) TiO_2 NPs treated normal colorectal cells NCM460, and colorectal cancer cells SW480 and Caco-2 at varying concentrations for 24h. Data are mean ± SD, n=3, One-way ANOVA Tukey post-hoc HSD, * states the significant difference between the sample groups and the negative control. p<0.05.

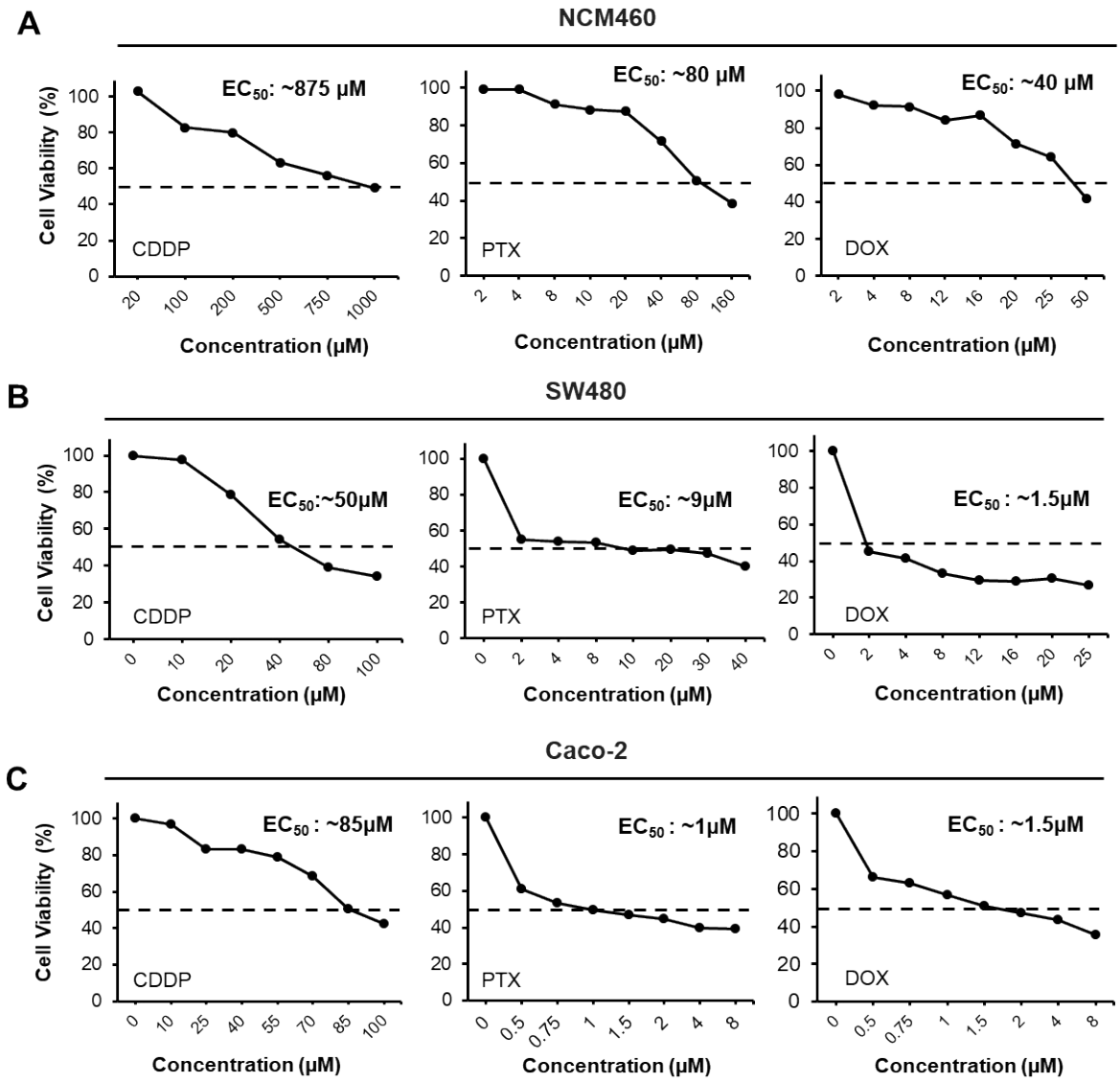

Figure S2. Dose response profile following anticancer drugs treatment (24h) in (A) NCM460 (B) SW480 and (C) Caco-2 cells. Half maximal effective concentration (EC_{50}) of each drug for the cell lines are noted on the graphs.

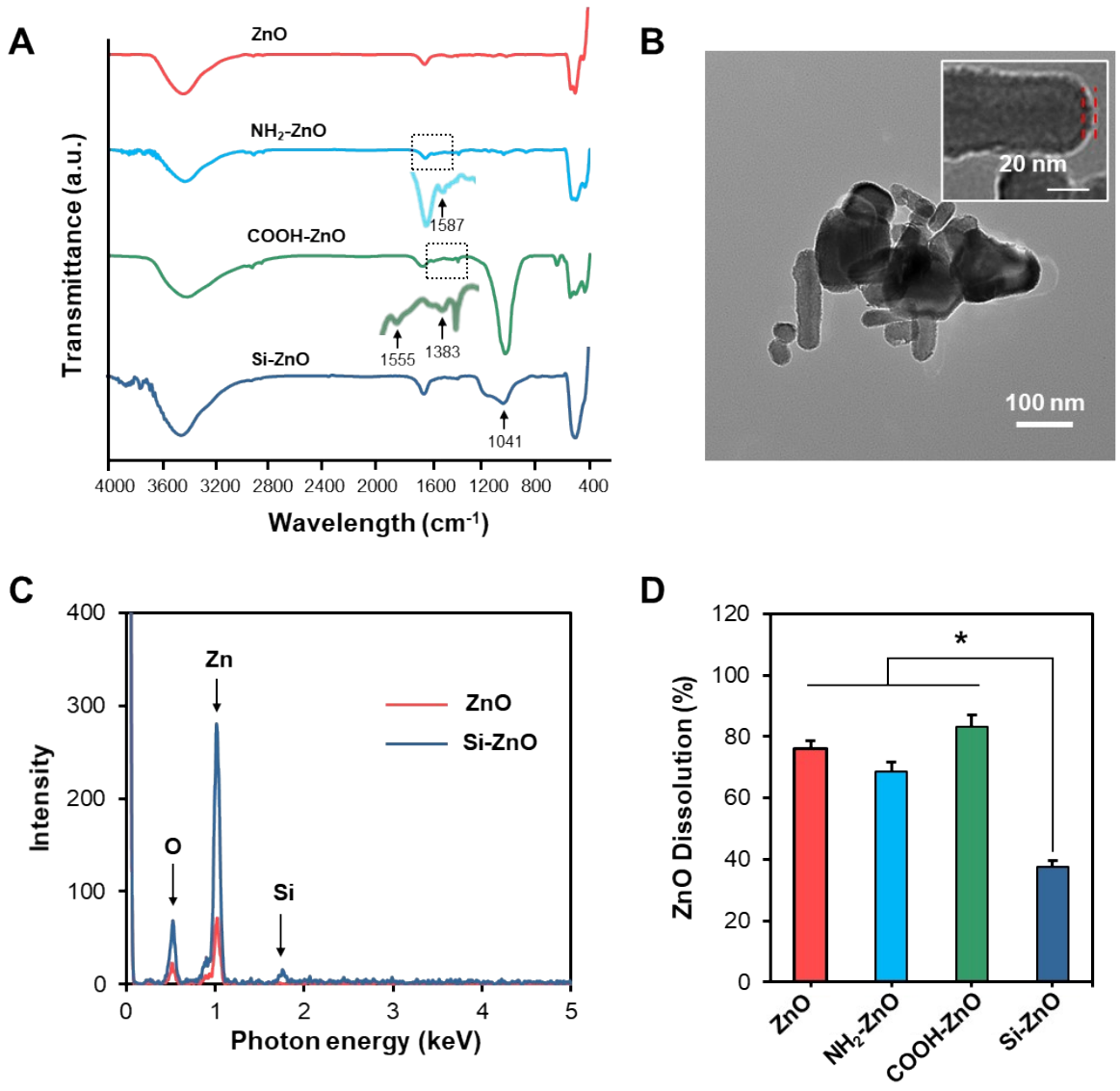

Figure S3. Physical characterization of the pristine ZnO, amine-functionalized (NH_2-ZnO), carboxylic acid functionalized (COOH-ZnO) and silica coated (Si-ZnO) NPs. (**A**) FTIR spectra of the ZnO NPs variants showing the respective characteristic peaks. (**B**) Representative TEM image of Si-ZnO depicting the presence of thin silica coat (~5.6 nm). (**C**) EDX spectra of ZnO and Si-ZnO NPs revealed successful coating of the silica shell onto the core ZnO NPs. (**D**) *in vitro* dissolution of the ZnO NPs at the lysosomal environment (pH 4.7). Data presented are mean ± S.D., n=3, One-way ANOVA Tukey post-hoc HSD, * states the significant difference between the indicated ZnO NP variants and the Si-ZnO NP group. $p<0.05$.

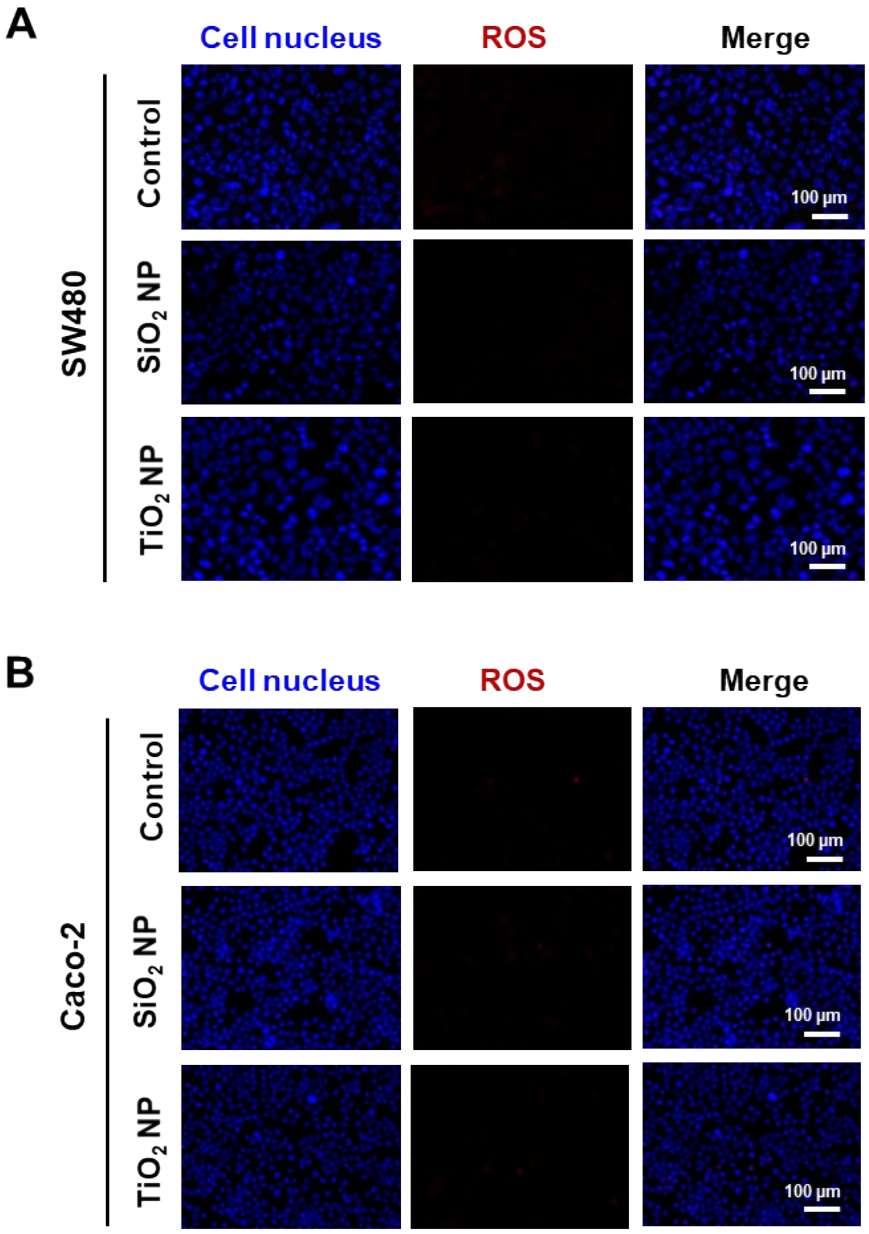

Figure S4. Representative fluorescence images of SiO_2 and TiO_2 NPs treated (A) SW480 and (B) Caco-2 cells counterstained for the cell nucleus (blue) and intracellular ROS (red).

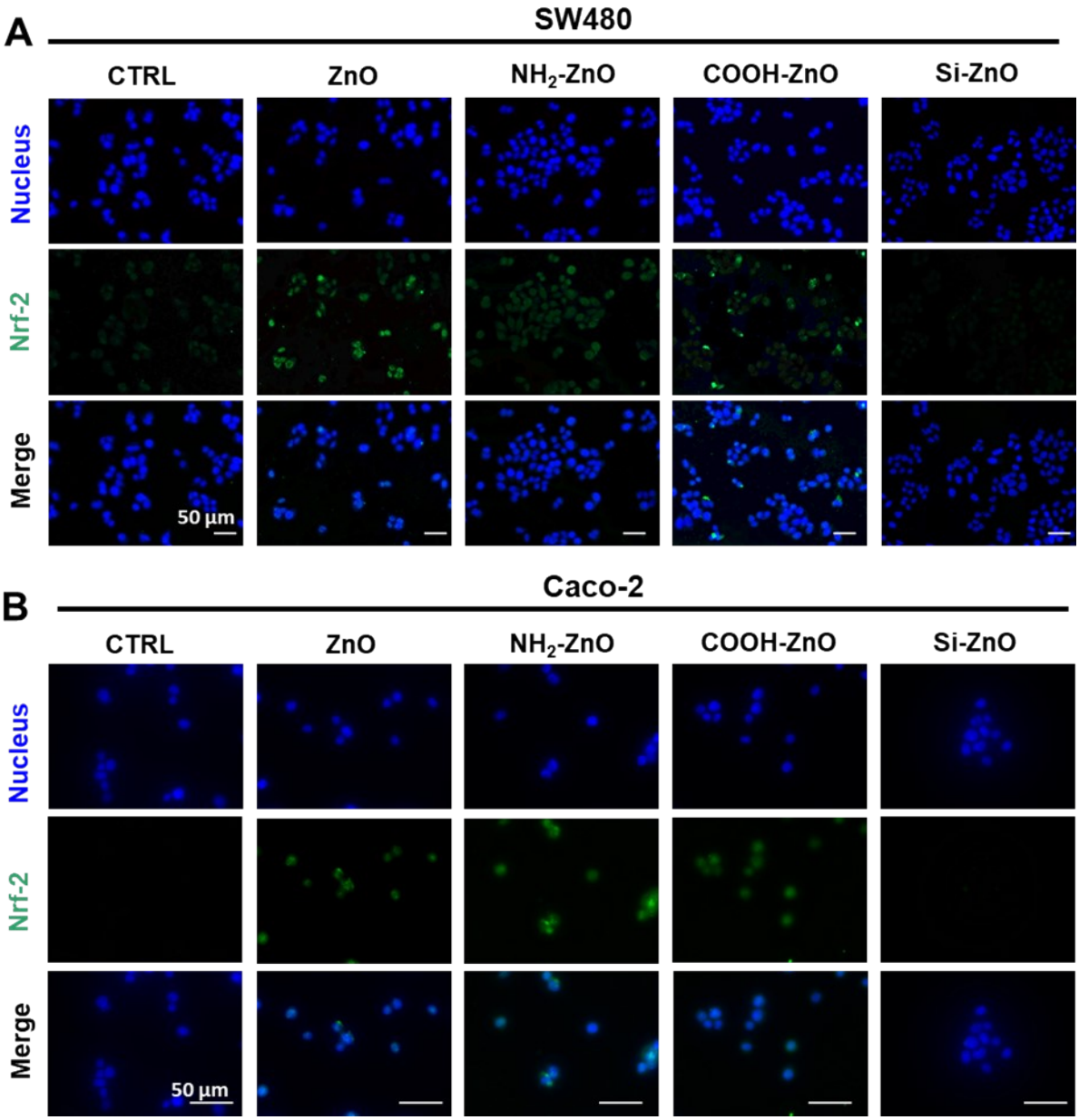

Figure S5. ZnO NPs induced increase expression of Nrf2. Representative immunofluorescence images of (A) SW480 and (B) Caco-2 cells counterstained for Nrf2 (green) and cell nucleus (blue) following their exposure to the ZnO NPs (20 µM, 4h). Scale bar = 50 µm.

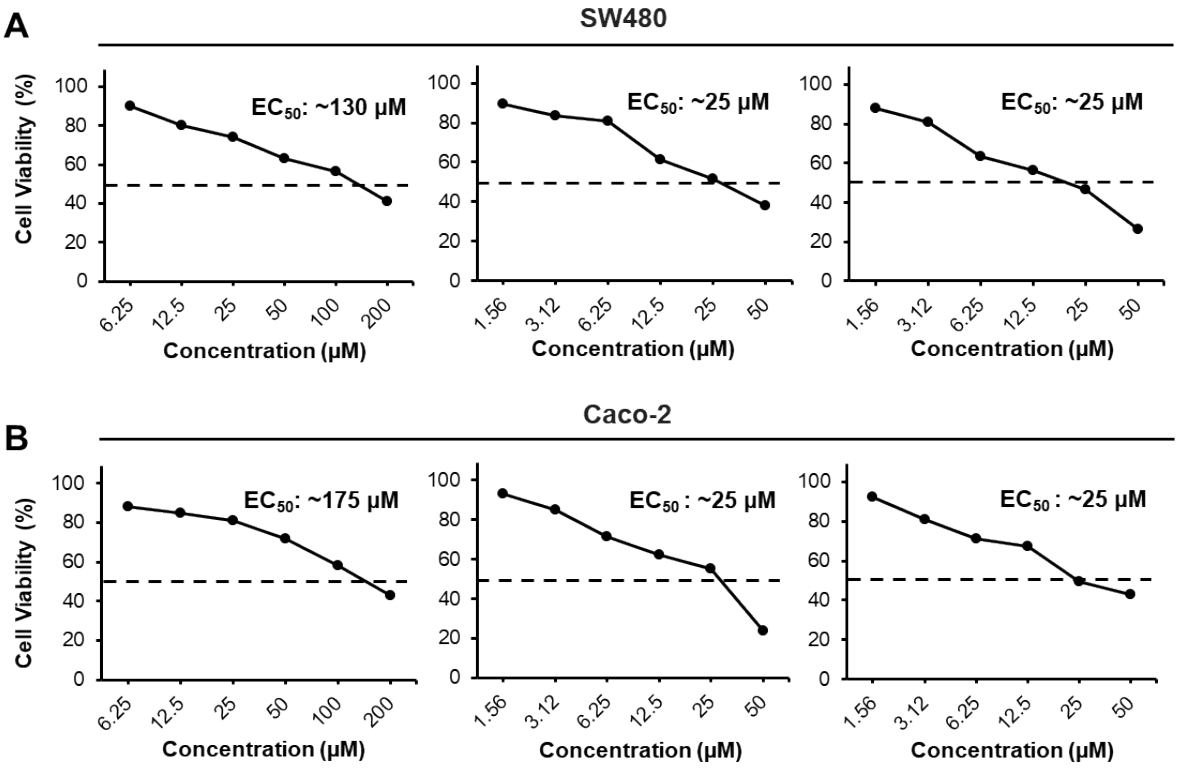

Figure S6. Dose response profile following anticancer drugs treatment (24h) in (**A**) SW480 and (**B**) Caco-2 tumor spheroids. Half maximal effective concentration (EC_{50}) of each drug for the two tumor spheroids was noted on the graphs.